JOURNAL OF MARITIME RESEARCH

Vol XX. No. III (2023) pp 224–239

ISSN: 1697-4840, www.jmr.unican.es

Structural analysis of wind turbine blade by using finite element method

Kazi Naimul Hoque[1,*], Samin Abrar Chowdhury[1], Syed Assiqul Haque[1]

ARTICLE INFO

Article history:
Received 12 Sep 2023;
in revised from 26 Sep 2023;
accepted 18 Oct 2023.

Keywords:
Wind turbine blade, finite element analysis, composite materials, von-Mises stress, NACA 2412, strain energy.

ABSTRACT

Wind turbine serves as one of the reliable sources of renewable energy converter around the globe. The main purpose of the wind turbine is to extract maximum aerodynamic efficiency utilizing the wind and turbine blade acting as the main factor for harnessing wind energy. To ensure a turbine blade with required structural integrity as well as aerodynamically thin structure, blade material plays a vital role. The blade materials in a turbine blade should have properties like fatigue resistance, low density, and higher strength. In this study, wind turbine blades are designed using SolidWorks software and analysis is performed for six different materials using the finite element method. The materials used here are carbon epoxy, glass polyester, epoxy E-glass, epoxy S-glass, epoxy carbon UD (230 GPa) prepreg, and structural steel. The purpose of this analysis is to explore the nodal deformation and von-Mises stress distribution as well as maximum strain energy. Later, graphical, and tabular results are presented for the target elements, occurring at the most vulnerable region of blade structure. The results are also presented in terms of maximum von-Mises stress, maximum deformation, and total strain energy. The main goal of this study is to validate and compare the above-mentioned materials with conventional ones to select the best material for the wind turbine blade.

1. Introduction.

The wind energy conversion system (WECS) [1] includes wind turbines, generators and other apparatus which converts the kinetic energy from the wind velocity into mechanical energy. The wind turbine extracts kinetic energy by its rotating blade connected with a gear box usually with a high-speed ratio. This extracted mechanical energy is then converted into electrical energy by means of generator [2].

The main purpose of the wind turbine is to extract maximum aerodynamic efficiency utilizing the wind. The number of blades used in a wind turbine proportional to the aerodynamic efficiency. in this context if we increase the blade number from two to three our aerodynamic efficiency will increase approximately 3%. In contrast adding one more blade hardly increases the efficiency but increase the cost. That's why three blade serves an optimum design [3].

Blade acts as the main factor for harnessing wind energy. For maximum aerodynamic efficiency the blades are required to be thin while for structural integrity thick blades are preferable. Also, turbine blades are affected significantly by external forces such as flap and edge loading which triggers tensile and compressive stresses as well as deformation. Flap and edge bending is responsible for 97% of blade damage [4] [5].

To ensure a long and maintenance free life cycle stiffness, fatigue resistance and high strength are a must. Combining different composites materials for blade design both the dynamic and mechanical property can be modified to get the optimum design [6].

In this paper, finite element analysis is conducted for different composite materials on an existing wind turbine blade having airfoil design NACA 2412. Other design factors considered here are-

- For the symmetry of turbine blades, the analysis is conducted on one blade.
- For initial study, blades are considered to have no twist angle.

[1]Bangladesh University of Engineering and Technology.
[*]Corresponding author: Kazi Naimul Hoque. E-mail Address: kazinaim@name.buet.ac.bd.

- The wind velocity and load are uniform throughout the blade length.

2. Turbine blade geometry.

2.1. Blade.

Figure 1: Different parts of wind turbine blade.

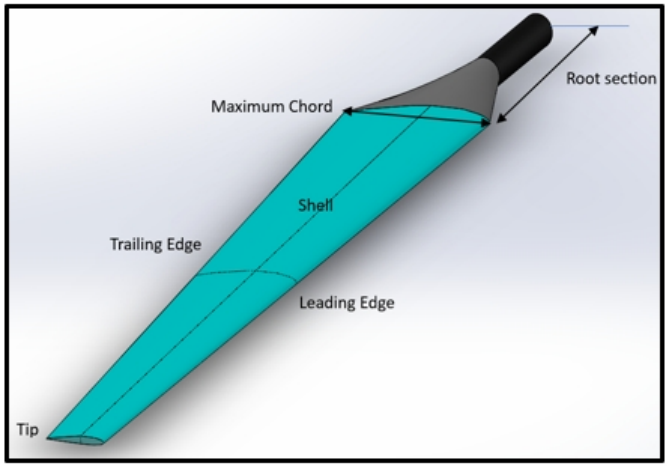

Source: Authors.

Figure 2: NACA 2412 airfoil.

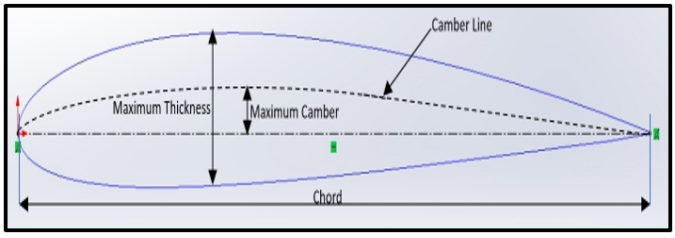

Source: Authors.

A wind turbine is a complex structure combining different parts working together to convert the wind energy efficiently. Fig. 1 denotes different parts of a modern wind turbine blade [7].

- Root section- The thick root section is attached to the hub of the turbine. This section is usually thicker than other parts to provide necessary structural strength to the blade. The main purpose is to transmit the rotational forces from blade to hub.
- Shear Web- It is one kind of web which rum along the length of the blade to provide structural rigidity.
- Airfoil section- Airfoil sections are used to shape the blade profile so that the blade profile can achieve proper aerodynamic property. The airfoil sections are designed such way that they generate lift which allows the blade to rotate.
- Shell or Plate- It covers the internal structures and provides aerodynamic shape to the blade as well as provides protection from environmental factors.
- Leading Edge- The front edge of the blade where the wind makes the first contact.
- Trailing Edge- The rare edge where the wind will pass after separating. It needs to be thin and smooth as possible to ensure minimum drag and maximum aerodynamic efficiency.
- Tip- The farthest point from the blade hub. This region moves at the highest velocity.

These above-mentioned parts are considered in this study. Apart from this, to generate a constant lift force with respect to the drag force, a certain twist is given to the blade which is not considered in this study.

2.2. Airfoil design.

The airfoil shape taken in this paper is NACA 2412, as shown in Fig. 2. This profile is developed by National Advisory Committee for Aeronautics (NACA). In general, NACA profiles are used in aviation. But due to their aerodynamic characteristics they ae being widely used as turbine blades [8].

The designation “NACA 2412” stands for-

- NACA- National Advisory Committee for Aeronautics, the organization that developed this profile.
- 2 – The first digit represents maximum camber as a percentage of the chord indicated in fig-2. Here, the maximum camber is 2% of the chord length.
- 4 – The second digit represents the location of maximum camber from the leading edge in ten percent of the chord. In this case it is located 40% from the leading edge.
- 12 – the last two digits represent the maximum thickness. Here it is 12% of the chord.

NACA 2412 is being used extensively in wind turbine blade design for having a good compromise between lift and drag. It can provide suitable lift while maintaining reasonable drag levels. Fig. 3 shows the cross-sectional view of turbine blade. In the case of NACA profile, when the wind passes, it creates a pressure difference between the upwind face and downwind face, resulting in lift force.

3. Composite materials.

A composite material is a combination of two or more materials having significantly different properties. Their combination results in better properties than any of the individual material [9] [10].

Figure 3: Cross-sectional view of wind turbine blade.

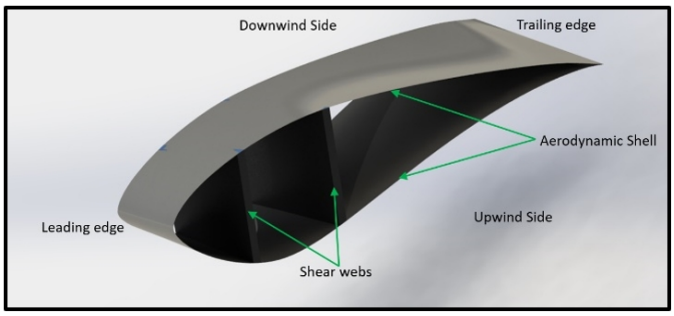

Source: Authors.

3.1. Advantages of composite materials.

Composite materials provide:

- Higer strength to weight and stiffness to weight ratio than conventional material.
- Better fatigue properties.
- Easier fabrication process for complex structural shapes like turbine blade.
- Higher resistance to impact damage and corrosion.
- Lighter weight and density.

In the above context, today's wind turbine is highly dependable on composite materials to ensure a long and maintenance free life cycle. The question still remains how those properties mentioned above will increase the performance level of wind turbine. To answer that, two factors have to be considered, that is-

1. The blade should be as light as possible because.
   - To lower the fatigue loads induced by gravity.
   - For better performance.
   - Easy transportation and installation.
2. The blade needs to be stiff because.
   - For preventing local or global buckling.
   - For preventing the collision between blade and turbine tower.
   - To withstand both wind and gravity loads. Gravity loads are function of material density hence the weight.

So, an optimization is necessary between the mass and stiffness. Less weight and more stiffness are needed with a balanced aerodynamic and structural integrity. That is the reason for using composite materials. Fig. 4 illustrates that, when considering a constant Young's modulus, composite materials exhibit lower density. Fig. 4 is called "Ashby Plot" [11].

Fig. 4 is governed by the following process.

Figure 4: Ashby plot for different materials [8].

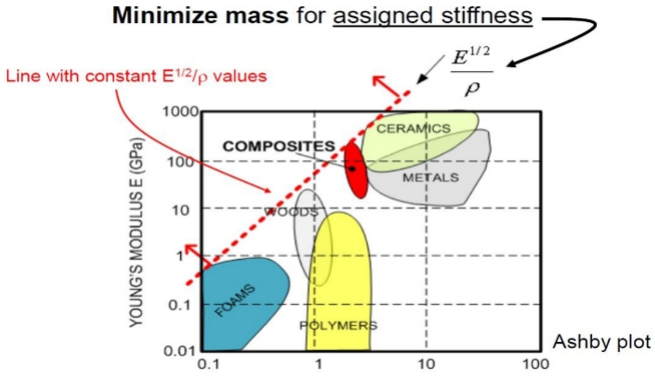

Source: Authors.

Figure 5: Mathematical interpretation of Ashby plot.

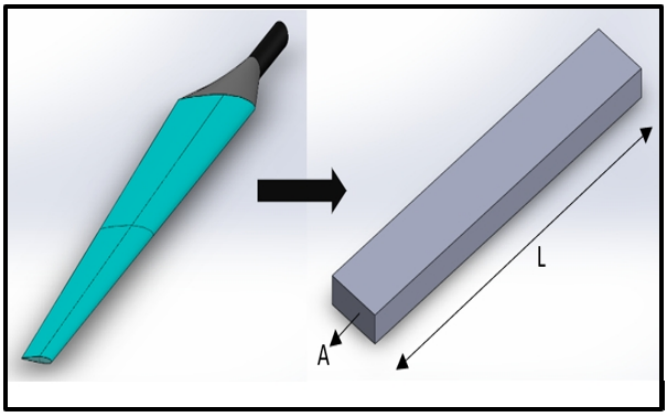

Source: Authors.

The assumption here is to consider the blade as a rectangular box of cross-sectional area 'A' and a length of 'L' which can be considered as a beam.

Mass of the beam, $M = AL\rho$

Stiffness of the beam, $S = F/\delta = KEI/L^3$

So, $M = (12S/KL)^{1/2} L^3(\rho/E^{1/2})$

From the above equation it is obvious that for a given stiffness, the mass is inversely proportional to $E^{1/2}/\rho$. For minimizing the mass, it is required to maximize $E^{1/2}/\rho$.

3.2. Commonly used composite materials in wind turbine blades.

- Carbon Fiber Reinforced Polymer (CFRP): Carbon fibers are incorporated into an epoxy-like polymer matrix. In comparison to fiberglass, CFRP has higher stiffness and strength, making it appropriate for larger and more sophisticated turbines.
- Fiberglass Reinforced Polymer (FRP): One of the most often utilized materials is this one. It is made up of glass fibers encased in a polymer matrix, typically polyester or epoxy resin. FRP is strong, long-lasting, and economically advantageous.

- Glass-Carbon Hybrid: These composite materials combine the advantages of carbon fiber and fiberglass. They offer a balance between price and quality.
- Epoxy Resins: Composites frequently use epoxy as their polymer matrix. It offers strong durability and resilience to external factors, as well as good adhesion to fibers.
- Polyester Resins: These resins offer sufficient mechanical qualities at a reasonable price for smaller wind turbine blades.

In this study, considering our blade size, wind condition, cost consideration; we have taken Carbon Epoxy Composite, Glass Polyester, Graphite Epoxy, E-glass UD, S-glass UD, Epoxy carbon Prepreg and Structural Steel for our analysis.

4. Finite element method.

The Finite Element Method (FEM) is a numerical technique used to solve complex engineering and mathematical problems [12]. It is especially beneficial for studying systems and structures with complex geometries, boundary conditions, and material characteristics. The general procedure is described below.

- Pre-processing step:

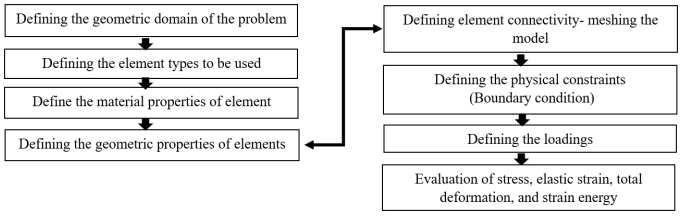

- Solution step: In this step, equations are solved using various numerical techniques such as matrix operations and iterative methods. The finite element program calculates the unknown values of the fundamental variables by assembling several governing algebraic equations in matrix form. To calculate other variables, the computed values are further substituted and computed.
- Post-processing step: After the solution step, valuable information can be extracted from the obtained results such as stress distribution, strain, deformation, strain energy and other parameters.

5. Governing equations.

From mathematical standpoint, [13] Finite Element Method (FEM) is a numerical method used for solving a set of related differential equations such as:

The global FEM equation relates the forces and moments acting on all of the mesh nodes (F), the displacements and rotations at all of the mesh nodes (U), that is, all of the degrees of freedom, and the global stiffness matrix (K).

$$[F] = [K]\{U\} \tag{1}$$

Here, the nodal forces [F] is filled with any of the known external loads and the nodal displacement {U} needs to be filled with boundary conditions.

- Stress Calculation:

In FEA, for linear analysis stress is often calculated using Hooke's law, which relates stress (σ) to strain (ε) through the material's elastic modulus (E):

$$\sigma = E{\cdot}\varepsilon \tag{2}$$

For nonlinear operations, FEA simulates the shear, tension, and bending stresses using complicated equations and empirical data. A set of vector equations are used in the software computations to describe how a component would behave under stress. The overall stress response is then created by combining the directional and deformation responses. The analysis's results can be expressed in terms of von-Mises stresses and elastic strains.

- Deformation Calculation:

Linear interpolation is typically used within elements to compute the displacement field.

- Energy Calculation:

In the context of FEA, there are different types of energies that can be calculated, such as strain energy and potential energy.

- Strain Energy:

The strain energy stored in a material due to deformation can be calculated using the formula:

$$U = 1/2 \int V\sigma \cdot \varepsilon \, dV \tag{3}$$

6. Loads on blades.

Wind turbine blades are subjected to various loads during their operation. For an efficient performance, it is crucial to understand the effects of these loads [14]. The primary loads on wind turbine blades include:

- Aerodynamic Loads: These are the loads that the wind itself produces. Wind turbine blades must be shaped like an airfoil to produce lift and drag forces in order to capture the kinetic energy of the wind. While the drag force works to prevent motion, the lift force is what propels the blades' rotation. These forces change according to wind direction and speed.
- Gravity Loads: Wind turbine blades are typically quite long and heavy, so they experience gravitational forces. These forces can lead to bending and twisting of the blade.

- Centrifugal Loads: Wind turbine blades experiences these loads due to their circular motion.
- Dynamic Loads: Due to variations in wind speed and direction dynamic load is created on blades.

The above-mentioned loads primarily act flap wise direction and edge wise direction on wind turbine blade.

Figure 6: Loads on blade.

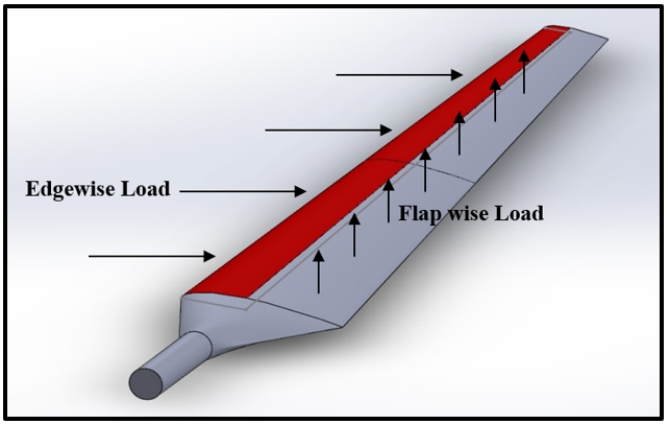

Source: Authors.

Flap wise load:

- Direction: It acts perpendicular to the plane of the blade rotation that is to the upwind part of the blade.
- Causes: Flap wise loads primarily results from aerodynamic forces including lift and drag force generated as wind flows over the airfoil shape blade.
- Effects: It leads to banding of the blade along the length.

Edge wise load:

- Direction: Acts perpendicular to flap wise direction. In this study, the load for edge area is assumed to occur throughout the 40% of total blade face area from the leading edge across the width of the blade. 40% area is taken according to the maximum thickness of the chosen airfoil section.
- Causes: Edge wise loads typically results from gravity and centrifugal forces due to blade's rotation.
- Effects: Edgewise loads can lead to twisting or torsional deformation of the blade.

7. Materials selection.

The properties of structural steel and composite materials are given below:

7.1. Structural steel.

The structural steel is most commonly used for construction of buildings, bridges, steel infrastructure and other industrial structure. It has a high weight to strength ratio, high ductility and quite durable and such characteristics make this material suitable for construction purpose.

Table 1: Properties of structural steel.

Density (g/cm^3)	7.85
Young's Modulus (GPa)	80
Poisson's Ratio	0.29
Shear Modulus	31.008
Tensile Stress (MPa)	450
Shear Stress (MPa)	515

Source: Authors.

7.2. Carbon epoxy.

A carbon epoxy composite, also known as a CFRP (Carbon Fiber Reinforced Polymer), is a high-performance material used in various industries, including aerospace, automotive, sports equipment, and construction. It is made by combining carbon fiber and an epoxy resin matrix.

Table 2: Properties of carbon epoxy .

Density (kg/m^3)	1446.2
Young's Modulus (MPa) E_x	1727
Young's Modulus (MPa) E_y	7200
Young's Modulus (MPa) E_z	7200
Poisson's Ratio v_{xy}	0.3
Poisson's Ratio v_{yz}	0.21
Poisson's Ratio v_{zx}	0.21
Modulus of Rigidity (MPa) G_{xy}	3760
Modulus of Rigidity (MPa) G_{yz}	3760
Modulus of Rigidity (MPa) G_{zx}	3760

Source: Authors.

7.3. Glass polyester.

Glass polyester, often referred to as fiberglass reinforced polyester (GRP), is a composite material composed of polyester resin and glass fibers. This combination results in a material that offers a balance of strength, durability, and corrosion resistance. It is widely used in boat hulls, and automobile parts.

7.4. Epoxy carbon UD (230 GPa) prepreg.

"Prepreg" is short for "pre-impregnated" composite material. It refers to a type of composite material that consists of reinforcement fibers that have been pre-impregnated or pre-coated with a thermosetting resin matrix. Prepregs are commonly used in aerospace, automotive, marine, and other industries where high-performance and precise control over material properties are required. That's why in this study prepreg epoxy carbon is taken.

Table 3: Properties of glass polyester.

Density (kg/m^3)	1960
Young's Modulus (GPa) E_x	48.16
Young's Modulus (GPa) E_y	11.21
Young's Modulus (GPa) E_z	11.21
Poisson's Ratio v_{xy}	0.27
Poisson's Ratio v_{yz}	0.096
Poisson's Ratio v_{zx}	0.096
Modulus of Rigidity (MPa) G_{xy}	4420
Modulus of Rigidity (MPa) G_{yz}	4420
Modulus of Rigidity (MPa) G_{zx}	9000

Source: Authors.

Table 4: Properties of epoxy carbon UD (230 GPa) prepreg.

Density (kg/m^3)	1490
Young's Modulus (GPa) E_x	121
Young's Modulus (gPa) E_y	8.6
Young's Modulus (GPa) E_z	8.6
Poisson's Ratio v_{xy}	0.27
Poisson's Ratio v_{yz}	0.4
Poisson's Ratio v_{zx}	0.27
Modulus of Rigidity (MPa) G_{xy}	4700
Modulus of Rigidity (MPa) G_{yz}	3100
Modulus of Rigidity (MPa) G_{zx}	4700

Source: Authors.

7.5. Epoxy E-glass UD.

An epoxy E-glass composite is a type of composite material that combines E-glass fibers (often referred to as electrical glass fibers) with an epoxy resin matrix. This combination results in a strong, durable, and versatile material with a wide range of applications in aerospace industries.

Table 5: Properties of epoxy E-glass UD.

Density (kg/m^3)	2600
Young's Modulus (GPa) E_x	85
Young's Modulus (GPa) E_y	14
Young's Modulus (GPa) E_z	14
Poisson's Ratio v_{xy}	0.23
Poisson's Ratio v_{yz}	0.4
Poisson's Ratio v_{zx}	0.23
Modulus of Rigidity (MPa) G_{xy}	5000
Modulus of Rigidity (MPa) G_{yz}	3600
Modulus of Rigidity (MPa) G_{zx}	4000

Source: Authors.

7.6. Epoxy S-glass UD.

An epoxy S-glass composite is a type of composite material that combines S-glass fibers with an epoxy resin matrix. This combination creates a high-performance material known for its exceptional strength, durability, and resistance to various environmental factors.

Table 6: Properties of epoxy S-glass UD.

Density (kg/m^3)	2495
Young's Modulus (GPa) E_x	93
Young's Modulus (GPa) E_y	11
Young's Modulus (GPa) E_z	11
Poisson's Ratio v_{xy}	0.23
Poisson's Ratio v_{yz}	0.4
Poisson's Ratio v_{zx}	0.23
Modulus of Rigidity (MPa) G_{xy}	5000
Modulus of Rigidity (MPa) G_{yz}	3900
Modulus of Rigidity (MPa) G_{zx}	5000

Source: Authors.

8. Results and Discussion.

8.1. Specifications of wind turbine blade.

The following Table 7 indicates the specifications of wind turbine blade.

Table 7: Specifications of wind turbine blade.

Profile	NACA 2412
Root Chord length	1651 mm
Length of blade	10700 mm
Hub length	1465 mm
Hub Diameter	337.5 mm
Tip Chord length	650 mm
Hub to neck length	1475 mm

Source: Authors.

8.2. Wind turbine blade model.

A 3D geometric model of wind turbine blade is generated in SolidWorks, as shown in Fig. 7.

Figure 7: Blade model.

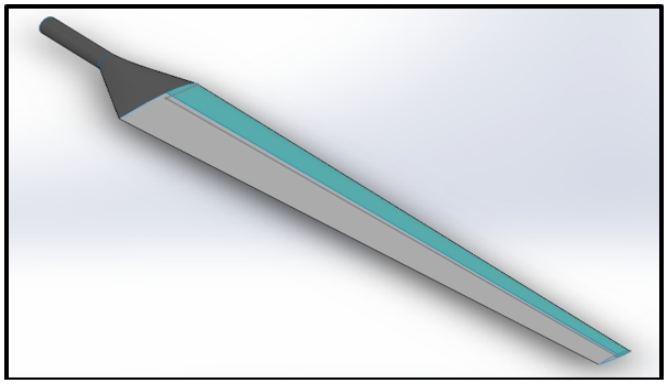

Source: Authors.

8.3. Load equation.

$$F = \pi \times \rho \times V^2 \times D^2 \tag{4}$$

Here,
P = Density = 1.29 Kg/m^3.

V = Wind Velocity = 10 m/s.
D = 30 m.
So, $F = \pi \times 1.29 \times 10^2 \times 30^2 = 364554$ N.

8.4. Boundary conditions.

The Hub of the blade is fixed. So, all six degrees of freedom are constrained here. Also, the displacement along X and Z axes are also constrained for the blade and thus only translatory motion is constrained in these directions. This condition was implied so that the blade itself does not deform along the direction of rotation and towards the center.

Figure 8: a) Fixed support; b) Displacement along X and Z axes are constrained.

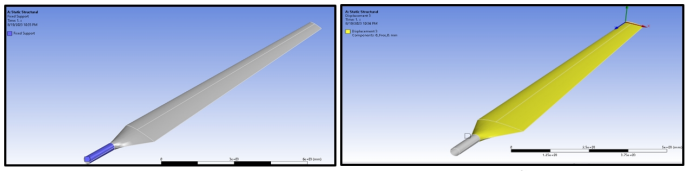

(a) (b)

Source: Authors.

8.5. Application of loadings.

For loading, pressure is applied on the edge area of the blade along X axis which is the direction of wind impact and pressure is applied normal to the flap area of the blade.

Edge wise pressure = 0.032842 MPa.
Flap wise pressure = 0.019288 MPa.

Figure 9: Application of flap wise pressure and edge wise pressure.

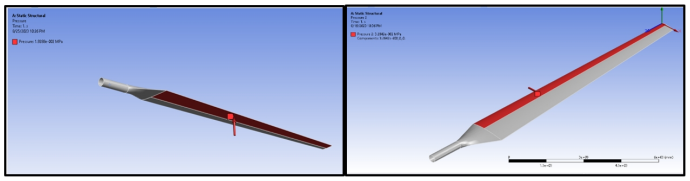

Source: Authors.

It is assumed that the pressure is uniform throughout the area for both flap area and edge area. The pressure for edge area is assumed to occur throughout the 40% of total blade face area from the leading edge and the rest is for flap area where flap wise pressure load is given.

8.6. Meshing.

The entire meshing is done in three parts. Mapped face meshing is generated in each part. The element size for Part A, Part B, Part C; are respectively 0.1m, 0.25m, 0.20m. Quadrilateral method is used for these face meshing. Also, quadrilateral dominant method is used for the entire body with quadratic element order. For the mesh metric of element quality, the max. is 0.99804, the min. is 5.0013e-002, the average is 0.52025 and the standard deviation is 0.27388. The total number of nodes is 16744 and elements are 5566.

Figure 10: Mesh generation of wind turbine blade.

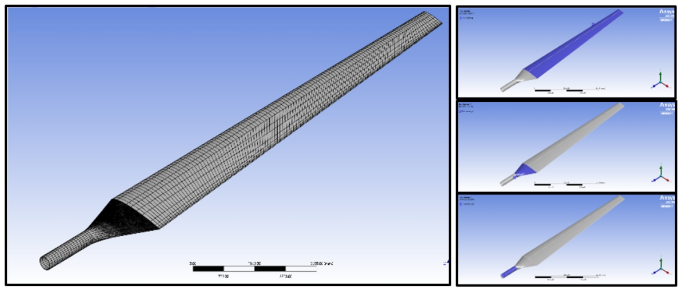

Source: Authors.

8.7. Analysis results.

8.7.1. Structural steel.

Figure 11: Total deformation and von-Mises stress distribution of structural steel.

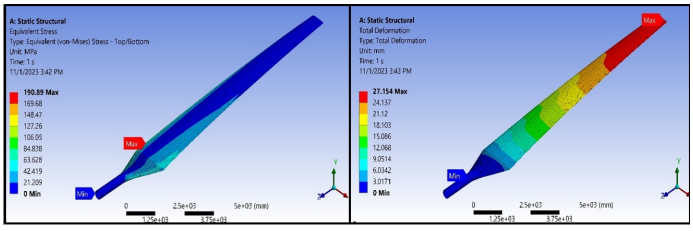

Source: Authors.

Figure 12: Total strain energy distribution of structural steel.

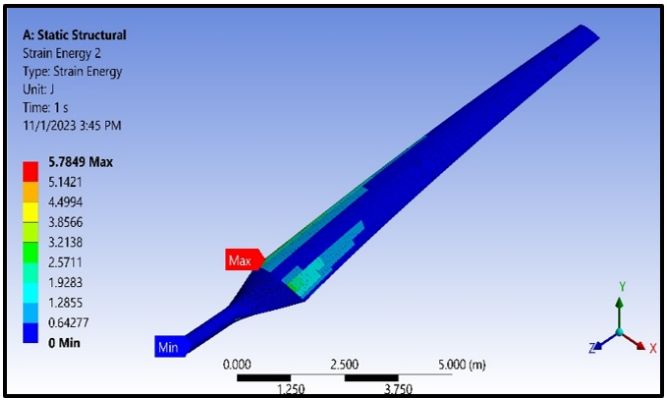

Source: Authors.

The maximum deformation is 27.154 mm, and it occurs at the tip of the blade. The maximum von-Mises stress is 190.89 MPa. Two elements were taken around the node of maximum deformation (Element no 3980 & 4102) and maximum stress (Element no. 3364 & 3365).

The maximum strain energy is 5.7849 J at element no. 3367 and the total Strain Energy is 1341.3 J. The elements and their corresponding nodes are marked in the figure 13 which were taken for nodal analysis. For each element, nodes were taken anti-clockwise and started from the bottom left node, as shown in Table 8.

Figure 13: a) Von-Mises stress distribution to the corresponding nodes (Element No. 3364 & 3365); b) Total deformation to corresponding nodes (Element No. 3980 & 4102).

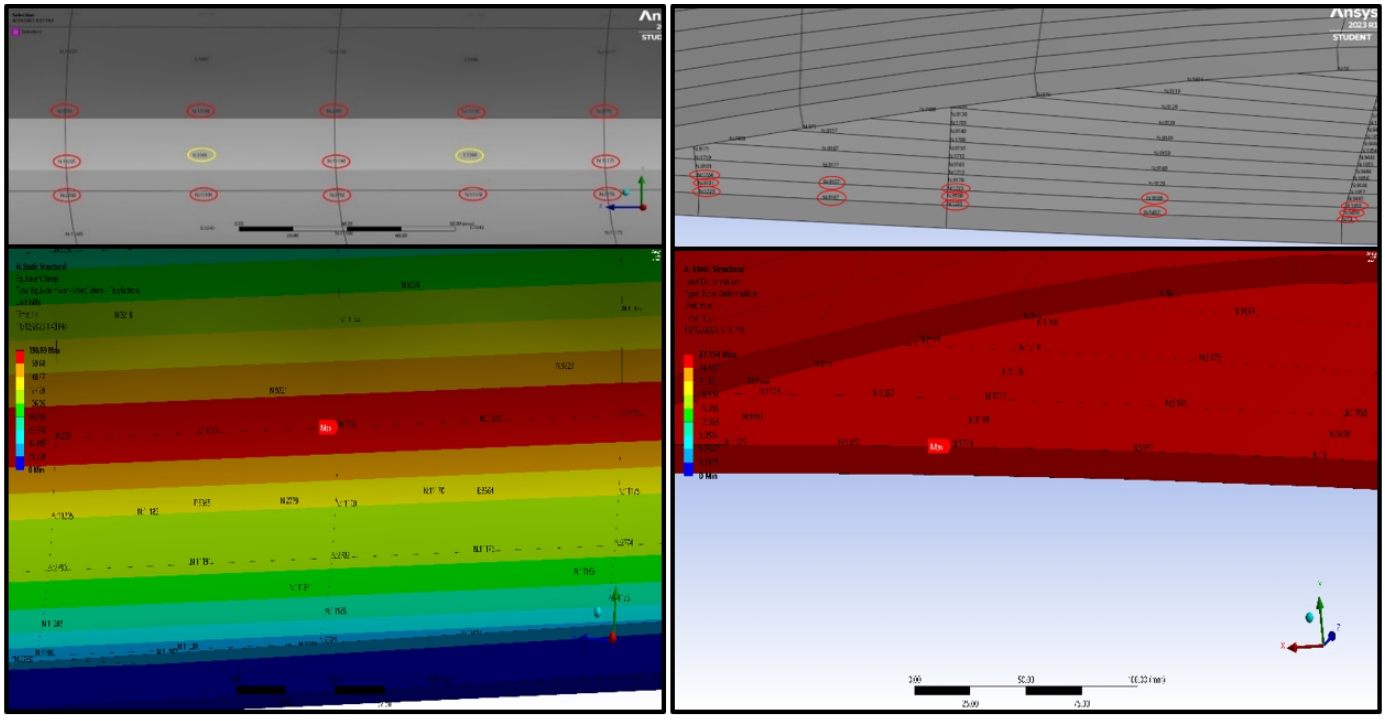

(a) (b)

Source: Authors.

Table 8: Element no. and corresponding node no. at the most vulnerable region of structural steel.

Element	Nodes							
3364	2782	11176	2774	11175	2775	11178	2783	11190
3365	2790	11191	2782	11190	2783	11193	2791	11205
3980	1728	5657	19	5658	1858	9189	1723	9188
4102	1729	9197	1728	9188	1723	9187	1724	9191

Source: Authors.

Figure 14: Total deformation, von-Mises stress and strain energy distribution of carbon epoxy.

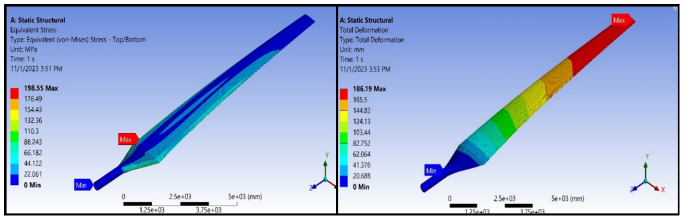

Source: Authors.

The maximum deformation is 186.19 mm, and it occurs at the tip of the blade. The maximum von-Mises stress is 198.55 MPa. Two elements were taken around the node of maximum deformation (Element no 3980 & 4102) and maximum stress (Element no. 3366 & 3367).

Figure 15: Strain energy distribution of carbon epoxy.

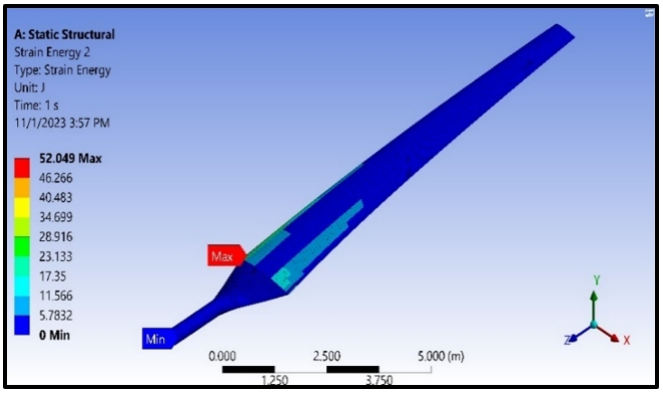

Source: Authors.

The maximum strain energy is 52.049 J at element no. 3368 and the total strain energy is 9301.5 J. Max. stress occurs at node no. 2799 & max. deformation occurs at node no. 1728. The elements and their corresponding nodes are marked in the figure 16 which were taken for nodal analysis. For each element, nodes were taken anti-clockwise and started from the bottom left node shown in Table 9.

Figure 16: a) Von-Mises stress distribution to the corresponding nodes (Element No. 3366 & 3367); b) Total deformation to corresponding nodes (Element No. 3980 & 4102).

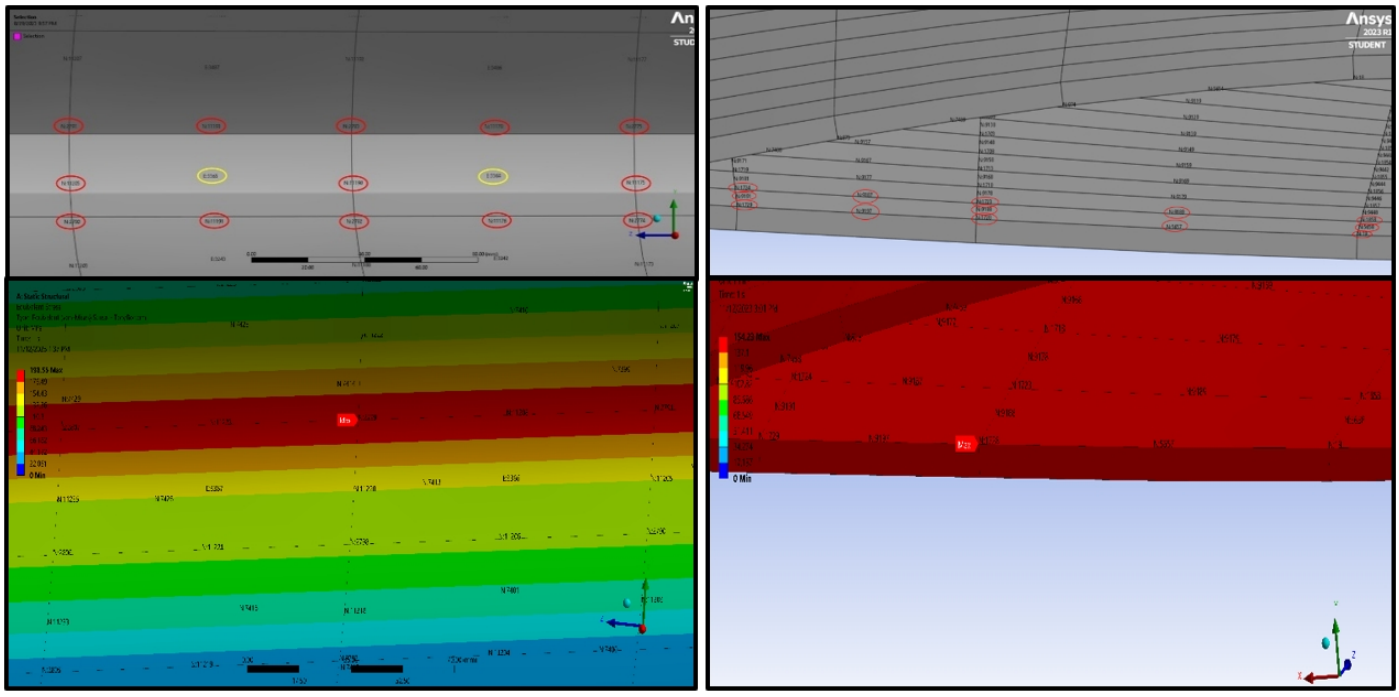

(a) (b)

Source: Authors.

Table 9: Element no. and corresponding node no. at the most vulnerable region of carbon epoxy.

Element	Nodes							
3366	2798	11206	2790	11205	2791	11208	2799	11220
3367	2806	11221	2798	11220	2799	11223	2807	11235
3980	1728	5657	19	5658	1858	9189	1723	9188
4102	1729	9197	1728	9188	1723	9187	1724	9191

Source: Authors.

8.7.2. Glass polyester.

Figure 17: Total deformation and von-Mises stress distribution of glass polyester.

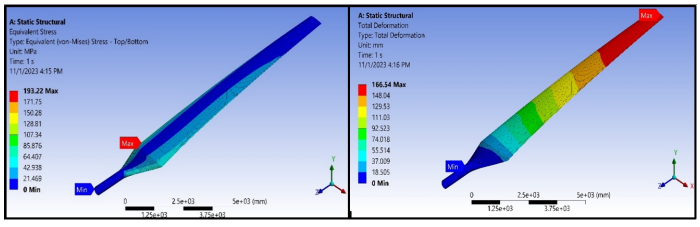

Source: Authors.

The maximum deformation is 166.54 mm, and it occurs at the tip of the blade. The maximum von-Mises stress is 193.22 MPa. Two elements were taken around the node of maximum deformation (Element no 3980 & 4102) and maximum stress (Element no. 3366 & 3367).

Figure 18: Total strain energy distribution of glass polyester.

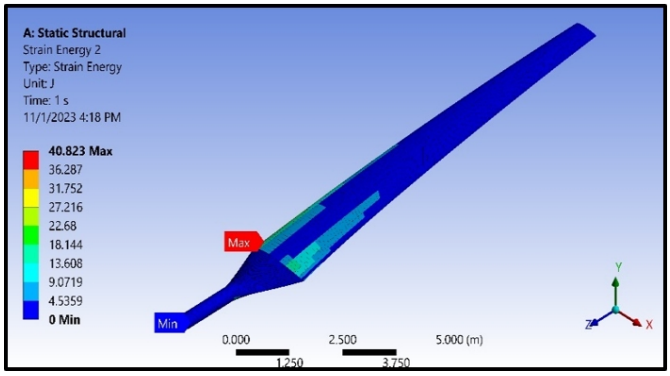

Source: Authors.

The maximum strain energy is 40.823 J at element no. 3367 and the total strain energy is 8221.9 J. Max. stress occurs at node no. 2799 & max. deformation occurs at node no. 1728. The elements and their corresponding nodes are marked in the figure 19 which were taken for nodal analysis. For each element, nodes were taken anti-clockwise and started from the bottom left node, as shown in Table 10.

Figure 19: a) Von-Mises stress distribution to the corresponding nodes (Element No. 3366 & 3367); b) Total deformation to corresponding nodes (Element No. 3980 & 4102).

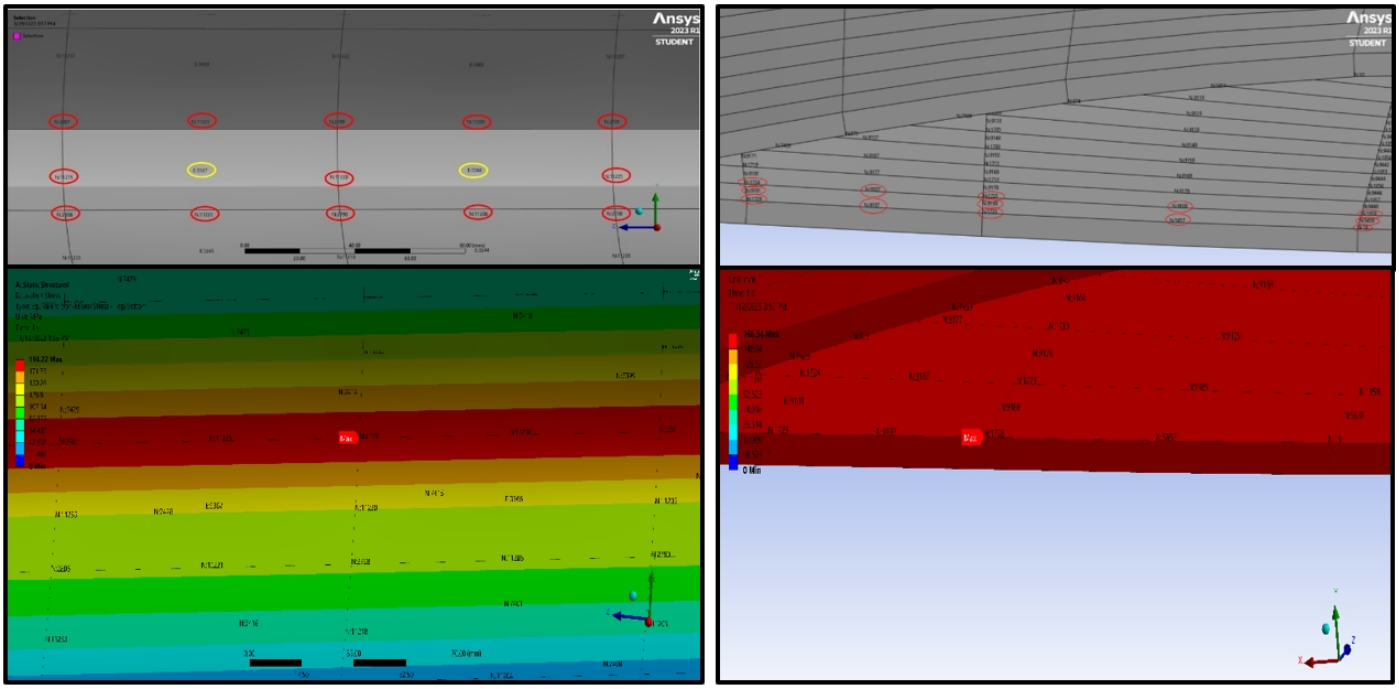

Source: Authors.

Table 10: Element no. and corresponding node no. at the most vulnerable region of glass polyester.

Element	Nodes							
3366	2798	11206	2790	11205	2791	11208	2799	11220
3367	2806	11221	2798	11220	2799	11223	2807	11235
3980	1728	5657	19	5658	1858	9189	1723	9188
4102	1729	9197	1728	9188	1723	9187	1724	9191

Source: Authors.

8.7.3. Epoxy E-glass UD.

Figure 20: Total deformation and von-Mises stress distribution of epoxy E-glass UD.

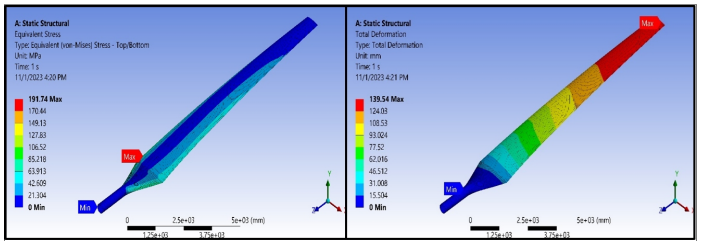

Source: Authors.

The maximum deformation is 139.54 mm, and it occurs at the tip of the blade. The maximum von-Mises stress is 191.74 MPa. Two elements were taken around the node of maximum deformation (Element no 3980 & 4102) and maximum stress (Element no. 3366 & 3367).

Figure 21: Total strain energy distribution of epoxy E-glass UD.

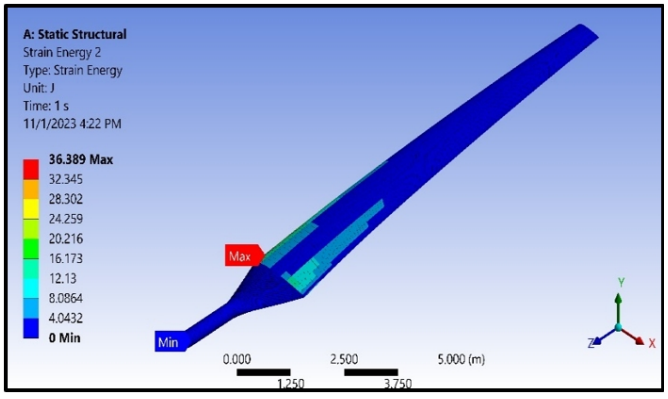

Source: Authors.

The maximum Strain Energy is 36.389 J at element no. 3367 and the total strain energy is 6955.6 J. Max. stress occurs at node no. 2799 & max. deformation occurs at node no. 1728. The elements and their corresponding nodes are marked in Fig. 22, which were taken for nodal analysis. For each element, nodes were taken anti-clockwise and started from the bottom left node, as shown in Table 11.

Figure 22: a) Von-Mises stress distribution to the corresponding nodes (Element No. 3366 & 3367); b) Total deformation to corresponding nodes (Element No. 3980 & 4102).

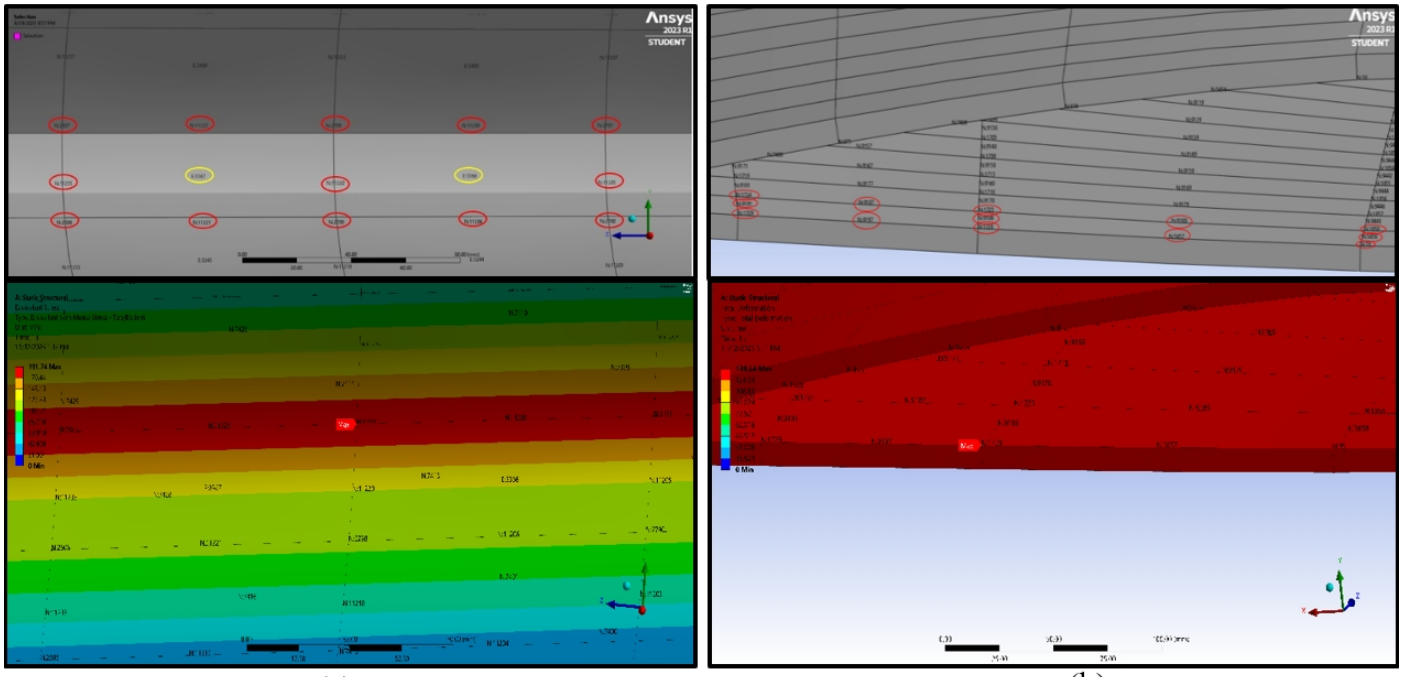

Source: Authors.

Table 11: Element no. and corresponding node no. at the most vulnerable region of epoxy E-glass UD.

Element	Nodes							
3366	2798	11206	2790	11205	2791	11208	2799	11220
3367	2806	11221	2798	11220	2799	11223	2807	11235
3980	1728	5657	19	5658	1858	9189	1723	9188
4102	1729	9197	1728	9188	1723	9187	1724	9191

Source: Authors.

8.7.4. Epoxy S-glass UD.

Figure 23: Total deformation and von-Mises stress distribution of epoxy S-glass UD.

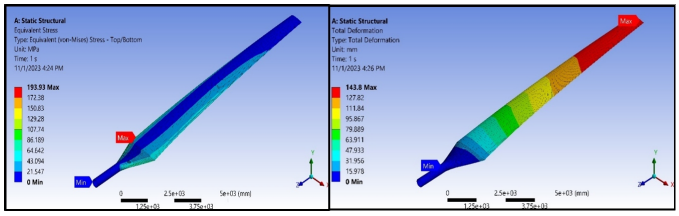

Source: Authors.

The maximum deformation is 143.8 mm, and it occurs at the tip of the blade. The maximum von-Mises stress is 193.93 MPa. Two elements were taken around the node of maximum deformation (Element no 3980 & 4102) and maximum stress (Element no. 3366 & 3367).

Figure 24: Total strain energy distribution of epoxy S-glass UD.

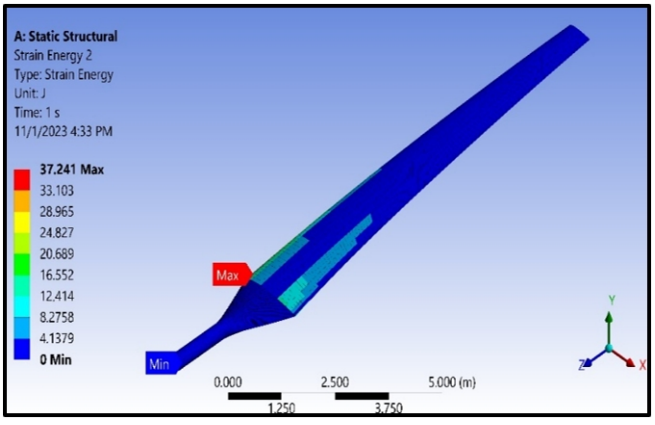

Source: Authors.

The maximum strain energy is 37.241 J at element no. 3367 and the total strain energy is 7137.9 J. Max. stress occurs at node no. 2799 & max. deformation occurs at node no. 1728. The elements and their corresponding nodes are marked in Fig. 25, which were taken for nodal analysis. For each element, nodes were taken anti-clockwise and started from the bottom left node, as shown in Table 12.

Figure 25: a) Von-Mises stress distribution to the corresponding nodes (Element No. 3366 & 3367); (b) Total deformation to corresponding nodes (Element No. 3980 & 4102).

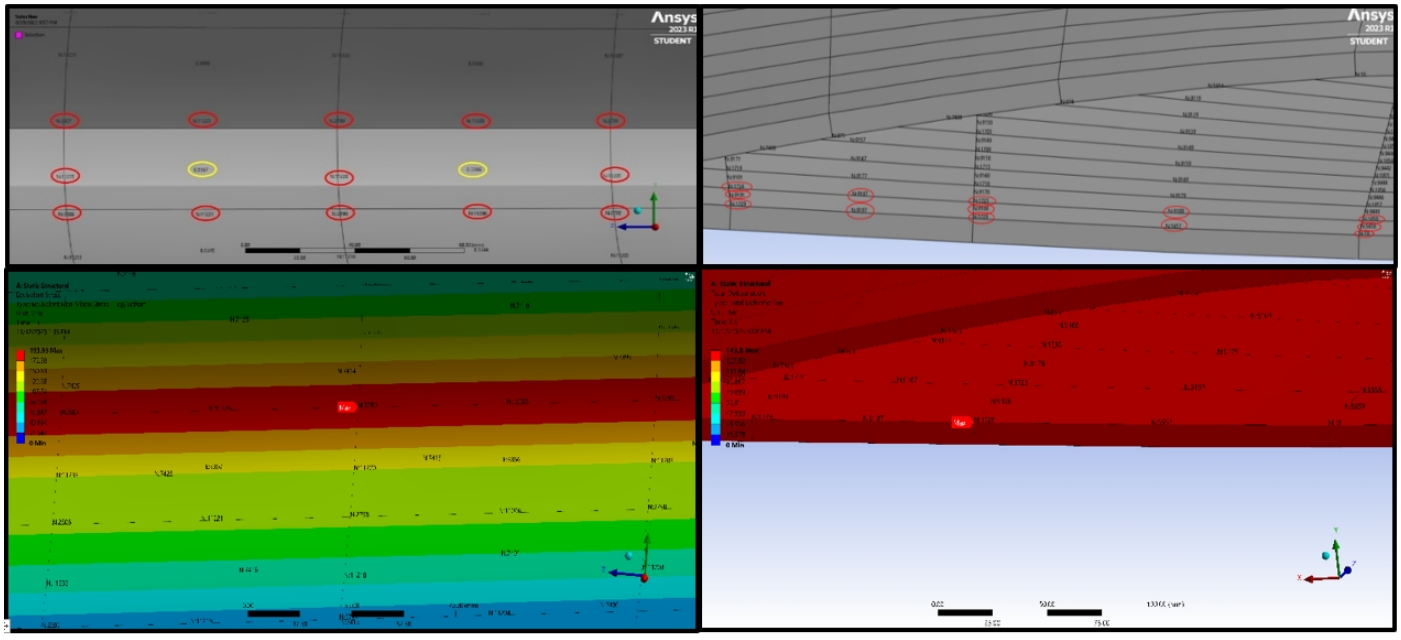

Source: Authors.

Table 12: Element no. and corresponding node no. at the most vulnerable region of epoxy S-glass UD.

Element	Nodes							
3366	2798	11206	2790	11205	2791	11208	2799	11220
3367	2806	11221	2798	11220	2799	11223	2807	11235
3980	1728	5657	19	5658	1858	9189	1723	9188
4102	1729	9197	1728	9188	1723	9187	1724	9191

Source: Authors.

8.7.5. Epoxy carbon UD (230 GPa) prepreg.

Figure 26: Total deformation and von-Mises stress distribution of epoxy carbon UD (230 GPa) prepreg.

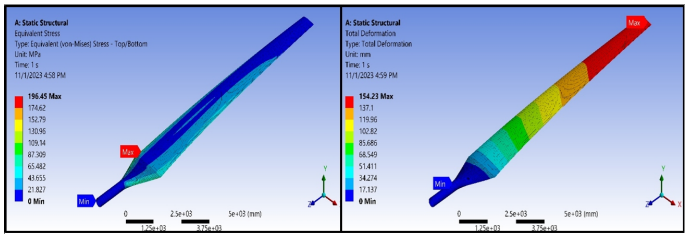

Source: Authors.

The maximum deformation is 154.23 mm, and it occurs at the tip of the blade. The maximum von-Mises stress is 196.45 MPa. Two elements were taken around the node of maximum deformation (Element no 3980 & 4102) and maximum stress (Element no. 3366 & 3367).

Figure 27: Total strain energy distribution of epoxy carbon UD (230 GPa) prepreg.

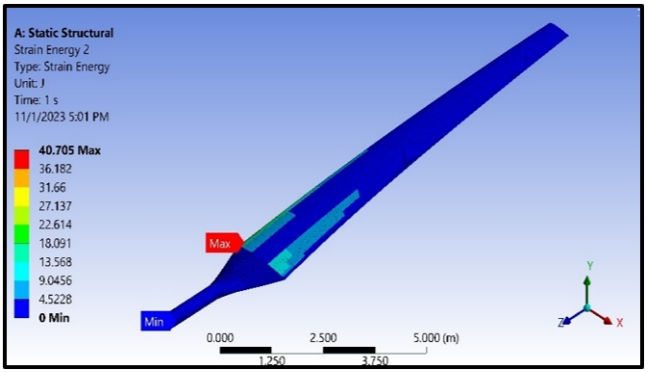

Source: Authors.

The maximum strain energy is 40.705 J at element no. 3367 and the total strain energy is 7644.7 J. Max. stress occurs at node no. 2799 & max. deformation occurs at node no. 1728. The elements and their corresponding nodes are marked in Fig. 28, which were taken for nodal analysis. For each element, nodes were taken anti-clockwise and started from the bottom left node, as shown in Table 13.

Figure 28: a) Von-Mises stress distribution to the corresponding nodes (Element No. 3366 & 3367); (b) Total deformation to corresponding nodes (Element No. 3980 & 4102).

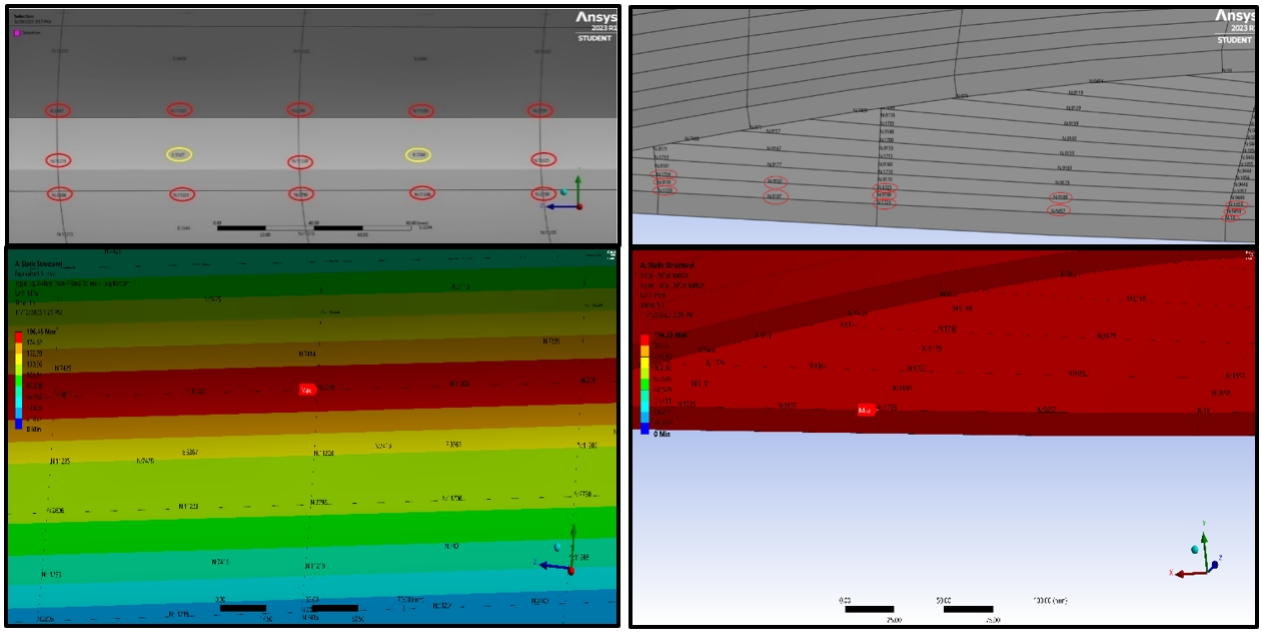

(a) (b)

Source: Authors.

Table 13: Element no. and corresponding node no. at the most vulnerable region of epoxy carbon UD (230 GPa) prepreg.

Element	Nodes							
3366	2798	11206	2790	11205	2791	11208	2799	11220
3367	2806	11221	2798	11220	2799	11223	2807	11235
3980	1728	5657	19	5658	1858	9189	1723	9188
4102	1729	9197	1728	9188	1723	9187	1724	9191

Source: Authors.

8.8. Graphical Analysis.

Figure 29: Comparison graph for average Von-Mises stress with standard deviation for the targeted elements of corresponding material.

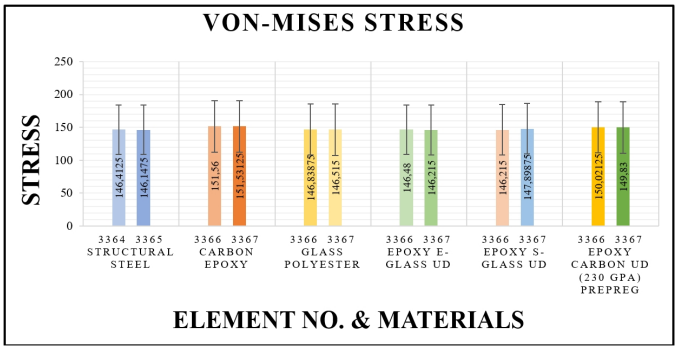

Source: Authors.

Graphical and tabular representation of the results are provided for the targeted elements of corresponding material, along with the average value of the outcome and their respective standard deviations. The outcomes are also compared for maximum von-Mises stress, maximum deformation, and total strain energy of different materials.

The two elements where maximum Von-Mises stress and maximum deformation occur are selected and the average stress of these elements for the corresponding material is plotted in Fig. 29 and the average deformation is plotted in Fig. 30. These figures are also accompanied by standard deviation. The average stress and the average deformation are found by taking the mean of stress and deformation found in the eight nodes respectively from analysis for corresponding elements of different materials.

Figure 30: Comparison graph for average deformation with standard deviation for the targeted elements of corresponding material.

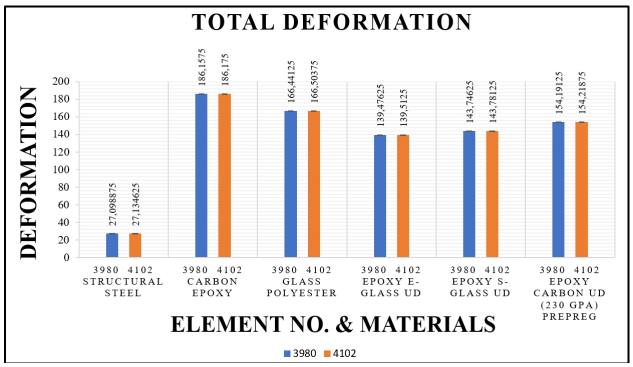

Source: Authors.

The values of average stress and average deformation for each element for corresponding materials and also the standard deviation for the corresponding outcomes is also tabulated in Table 14 and Table 15 giving a brief idea of how the outcome varies for different materials.

Table 14: Comparison of average stress and standard deviation of corresponding materials at their targeted elements.

Materials	Elements	Average stress (MPa)	Standard deviation (MPa)
Structural Steel	3364	146.41	37.21
	3365	146.14	37.38
Carbon Epoxy	3366	151.56	39.13
	3367	151.53	39.37
Glass Polyester	3366	146.84	38.89
	3367	146.52	39.07
Epoxy E-Glass UD	3366	146.48	37.83
	3367	146.22	38.01
Epoxy S-Glass UD	3366	148.15	38.26
	3367	147.89	38.44
Epoxy Carbon UD (230 GPa) Prepreg	3366	150.02	38.76
	3367	149.83	38.97

Source: Authors.

Table 15: Comparison of average deformation and standard deviation of corresponding materials at their targeted elements.

Materials	Elements	Average deformation (mm)	Standard deviation (mm)
Structural Steel	3980	27.09	0.06
	4102	27.13	0.02
Carbon Epoxy	3980	186.15	0.03
	4102	186.17	0.01
Glass Polyester	3980	166.44	0.11
	4102	166.50	0.03
Epoxy E-Glass UD	3980	139.47	0.06
	4102	139.51	0.02
Epoxy S-Glass UD	3980	143.74	0.05
	4102	143.78	0.01
Epoxy Carbon UD (230 GPa) Prepreg	3980	154.19	0.04
	4102	154.21	0.01

Source: Authors.

Table 16: Comparison of maximum von-Mises stress, maximum deformation & total strain energy for different composite materials.

Materials	Maximum von-Mises stress (MPa)	Maximum deformation (mm)	Total strain energy (J)
Structural Steel	190.89	27.154	1341.3
Carbon Epoxy	198.55	186.19	9301.5
Glass Polyester	193.22	166.54	8221.9
Epoxy E-Glass UD	191.74	139.54	6955.6
Epoxy S-Glass UD	193.93	143.8	7137.9
Epoxy Carbon UD (230 GPa) Prepreg	196.45	154.23	7644.7

Source: Authors.

The maximum Von-Mises stress, maximum deformation and total strain energy are tabulated in table 16 for each material. Also, the results graphically represented in figure 31 to obtain a more vivid outcome.

Figure 31: Comparison of maximum deformation, maximum stress, and total strain energy for different composite materials.

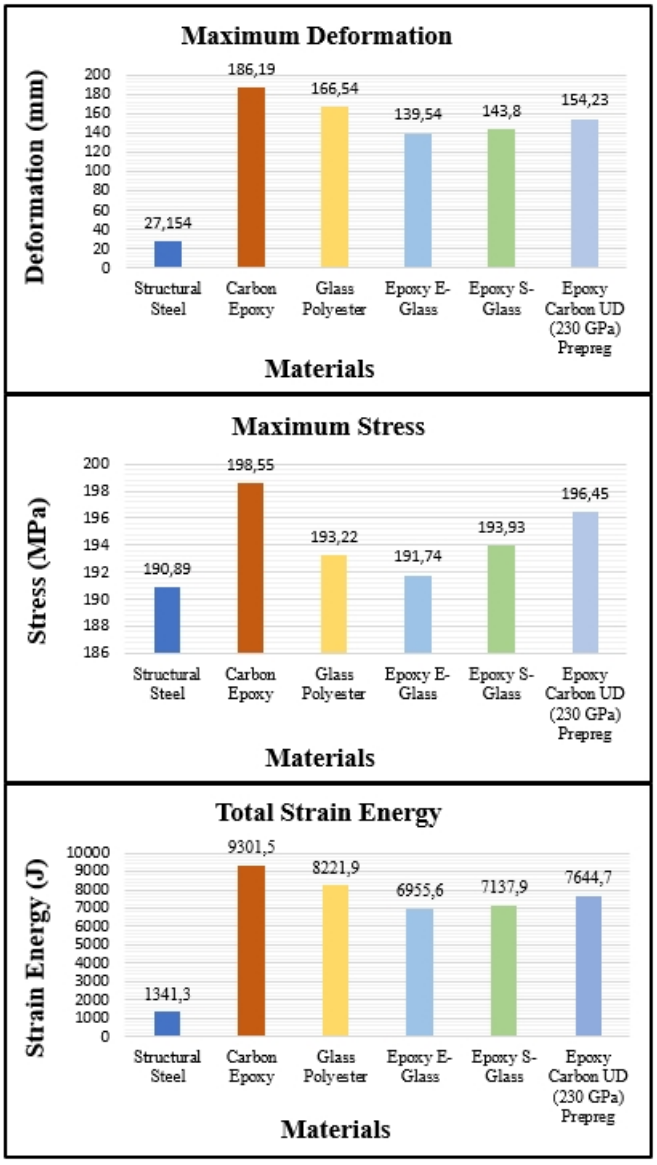

Source: Authors.

The graphical representation shows a more effective comparison between the materials. The maximum deformation and stress occur in Carbon Epoxy and the total strain energy is also maximum for this material. The minimum of these three occur in the case of structural steel. The optimum material requires a balance between these three characteristics.Analysis of turbine blade using composite materials also explored by Mathew et al. [8], Appadurai and Irudaya [15] and Diaaeldin et al. [16].

In [8] analysis on wind turbine blade is done using composite materials including Structural steel, E-glass, S-glass, Aluminum alloy and Epoxy-carbon considering isotropic properties. That is, they considered directional independence. In comparison, this study considers orthotropic properties of the used composite materials. Because composite materials show variation in their structural properties according to axial orientation.

In [15] analysis is done using carbon epoxy, graphite composite and steel varying impacted loads throughout the blade. In comparison, in this study load is applied segmenting the blade edge wise and flap wise for more accurate analysis.

In [16] six composite materials are implemented, and analysis results is concluded considering total deformation, Young's Modulus along axial direction and von-mises stress. While this study focuses on strain energy distribution along with other properties.

Now for this study, rather than using the whole blade geometry for analyzing different properties, nodal analysis is conducted. Most load impacted elements are taken and their nodal values for Deformation, Von-mises stress distribution is recorded. Then the analysis is taken one step further considering the Strain energy distribution along the blade as well. This micro level analysis as well as energy distribution will further be helpful in mesh convergence and reinforcing materials according to extremely affected zones.

The turbine blade used in this study is an existing one described in [8], so the analysis results follow the same trend in most cases as this study. Most importantly, this work has been able to show better deformation results using orthotropic analysis and considering strain energy for composite materials. Also, by segmenting the loading on flap wise and edge wise the result accuracy is increased.

Conclusions

An in-depth assessment was conducted using Ansys FEA to analyze the deformation, von-Mises stress, and maximum strain energy across five distinct composite materials in comparison to conventional structural steel.

For the conventional structural steel, the deformation and von-Mises stress is well acceptable whereas the strain energy is lesser compared to other materials. Glass Polyester, Epoxy E-Glass UD and Epoxy S-Glass UD shows approximately similar results in terms of von-Mises stress but Glass Polyester shows superiority in terms of strain energy where as in terms of deformation Epoxy E-Glass UD shows better result. But glass polyester shows relatively larger deformation. Except for carbon epoxy, the other materials exhibited relatively similar von-Mises stress values. Carbon epoxy has the largest total strain energy but also has the largest deformation and relatively large von-Mises stress which is not desirable. Epoxy Carbon UD (230 GPa) Prepreg shows better result than glass polyester in terms of deformation but has comparatively less strain energy than glass polyester.

Considering all three critical aspects—von-Mises stress, maximum deformation, and strain energy, it becomes apparent that Epoxy E-glass UD, Epoxy S-Glass UD and Epoxy Carbon UD (230 GPa) Prepreg have relatively balanced characteristics. Further research scope can be done considering a combination of these composite materials to find a much more optimum result of these three characteristics. Twist angle of the blade can also be introduced in the future study.

References.

[1] Rajveer Mittal, K.S.Sandhu and D.K.Jain, "An Overview of Some Important Issues Related to Wind Energy Conversion System (WECS)," International Journal of Environmental Science and Development, vol. 1, no. 4, pp. 351-363, October 2010.

[2] M. Jureczko, M. Pawlak and A. Mężyk, "Optimisation of wind turbine blades," Journal of Materials Processing Technology, vol. 167, no. 2-3, pp. 463-471, 2005.

[3] Asis Sarkar and Dhiren Kumar Behera, "Wind Turbine Blade Efficiency and Power Calculation with Electrical Analogy," International Journal of Scientific and Research Publications, vol. 2, no. 2, pp. 232-236, February 2012.

[4] Ole Thybo Thomsen, "Sandwich Materials for Wind Turbine Blades – Present and Future," Journal of Sandwich Structures and Materials, vol. 11, no. 1, pp. 7-26, January 2009.

[5] Meng-Kao Yeh and Chen-Hsu Wang, "Stress analysis of composite wind turbine blade by finite," in IOP Conference Series: Materials Science and Engineering, Tokyo, 2017.

[6] C. Kong, J. Bang and Y. Sugiyama, "Structural investigation of composite wind turbine blade considering various load cases and fatigue life," Energy, vol. 30, no. 11-12, pp. 2101-2114, 2005.

[7] M. E. Bechly and P. D. Clausent, "Structural Design of a Composite Wind Turbine Blade Using Finite Element Analysis," Computers & Structures, vol. 63, no. 3, pp. 639-646, May 1997.

[8] Akhil P Mathew, Athul S, Barath P and Rakesh S, "Structural Analysis of Composite Wind Turbine Blade" International Research Journal of Engineering and Technology (IRJET), vol. 05, no. 06, pp. 1377-1388, June 2018.

[9] Tri-Dung Ngo, Composite and Nanocomposite Materials: From Knowledge to Industrial Applications, London: IntechOpen, 2020.

[10] Rahul Reddy Nagavally, "Composite Materials - History, Types, Fabrication Techniques, Advantages, And Applications," in Proceedings of 29th IRF International Conference, India, 2016.

[11] Darshil U. Shah, "Natural fibre composites: Comprehensive Ashby-type materials selection charts," Materials and Design, vol. 62, pp. 21-31, October 2014.

[12] Sarah David Müzel, Eduardo Pires Bonhin, Nara Miranda Guimarães and Erick Siqueira Guidi, "Application of the Finite Element Method in the Analysis of Composite Materials: A Review," Polymers, vol. 12, no. 4, p. 818, April 2020.

[13] P. D. E. a. t. F. E. Method, Pavel Ŝolín, Canada: Wiley, 2005.

[14] Amna Algolfat, Weizhuo Wang and Alhussein Albarbar, "Dynamic Response Analysis of A 5 MW NREL Wind Turbine Blade under Flap-Wise and Edge-Wise Vibrations," Journal of Dynamics, Monitoring and Diagnostics, vol. 1, no. 4, pp. 208-222, September 2022.

[15] M. Appadurai and E. Fantin Irudaya, "Finite Element Analysis of Composite Wind Turbine," in International Conference on Electrical Energy Systems (ICEES), Chennai, 2021.

[16] Diaaeldin M. Elsherif, Ayman A. Abd El-Wahab, Ramadan Badawy Mohamed Elgamsy and Mohamed Hazem Abdellatif, ”Material Selection Of Wind Turbine Blade Using Finite Element Method,”International Journal of Scientific & Technology Research, vol. 8, no. 01, pp. 22-32, January 2019.

[17] Irshadhussain I. Master, Azim Aijaz Mohammad and Ratnesh T. Parmar, ”Aerodynamic Performance Evaluation of a Wind Turbine Blade by Computational and Experimental Method,” International Journal of Engineering Research & Technology (IJERT), vol. 3, no. 6, pp. 73-81, June 2014.

[18] S. K. Mutkule, P. P. Gorad, S. R. Raut and A. H. Nikam, ”Optimum and Reliable Material for Wind Turbine,” International Journal of Engineering Research & Technology (IJERT), vol. 4, no. 02, pp. 624-627, February 2015.